CONF-9010209--4

LA-UR- 90-3516

Los Alamos National Laboratory is operated by the University of California for the United States Department of Energy under contract W-7405-ENG-36.

LA-UR--90-3516

DE91 001965

TITLE: CONFINEMENT AND HEATING STUDIES OF FIELD-REVERSED CONFIGURATIONS

AUTHOR(S): CHRIEN, R. E.

SUBMITTED TO: IEA WORKSHOP ON PHYSICS OF ALTERNATIVE MAGNETIC CONFINEMENT SCHEMES
Villa Monastero
Varenna, ITALY
October 15-24, 1990

DISCLAIMER

Los Alamos National Laboratory
Los Alamos, New Mexico 87545

FORM NO. 836 R4
ST. NO. 2629 5/81

CONFINEMENT AND HEATING STUDIES OF FIELD-REVERSED CONFIGURATIONS

Robert E. Chrien

Los Alamos National Laboratory, Los Alamos, NM, USA

Abstract

Confinement studies of field-reversed configurations (FRCs) have been actively pursued during the past ten years with the larger and longer-lived FRCs produced in the FRX-C and FRX-C/LSM devices. Confinement measurements have included the global FRC quantities and, in some cases, profiles of electron temperature and density. The inferred confinement times and transport coefficients are used for comparison with transport models as well as to find the best operating conditions in the experiment.

Global power flow modelling shows that energy confinement during the equilibrium phase is usually dominated by particle losses, with a substantial secondary contribution from electron thermal conduction. Particle losses in present kinetic FRCs are strongly influenced by open field line confinement, which complicates the study of transport mechanisms. The electron thermal conduction is observed to be anomalous, as in other plasma devices. The bulk electrical resistivity is also anomalous and shows no evidence of classical Spitzer scaling. Recently, the resistive anomaly has been shown to correlate with tilt-like magnetic perturbations observed with Mirnov coils.

FRC confinement studies have also been extended to a higher temperature regime during magnetic compression heating. In these experiments, translated FRCs are compressed by increasing the external magnetic flux up to a factor of seven on a time scale between the radial Alfvén time and the FRC lifetime. Electron and ion temperatures up to 0.4 keV and 1.6 keV, respectively, have been obtained. Confinement times scale roughly as r^2 during compression.

I. Introduction

Field-reversed configurations are prolate compact toroids which have attracted interest within the magnetic fusion community because of their potential reactor advantages, including inherently high-β equilibria, simple cylindrical geometry, ease of translation, and a natural divertor. Although FRCs have been produced since the earliest days of magnetic fusion research, confinement studies have mainly been pursued during the past ten years after FRCs, free from various gross instabilities, began to be formed in the mid-1970's. An excellent review of FRC research was recently published;[1] a complete list of references can be found therein.

A schematic view of the FRC is shown in Figure 1. FRCs are formed within a theta

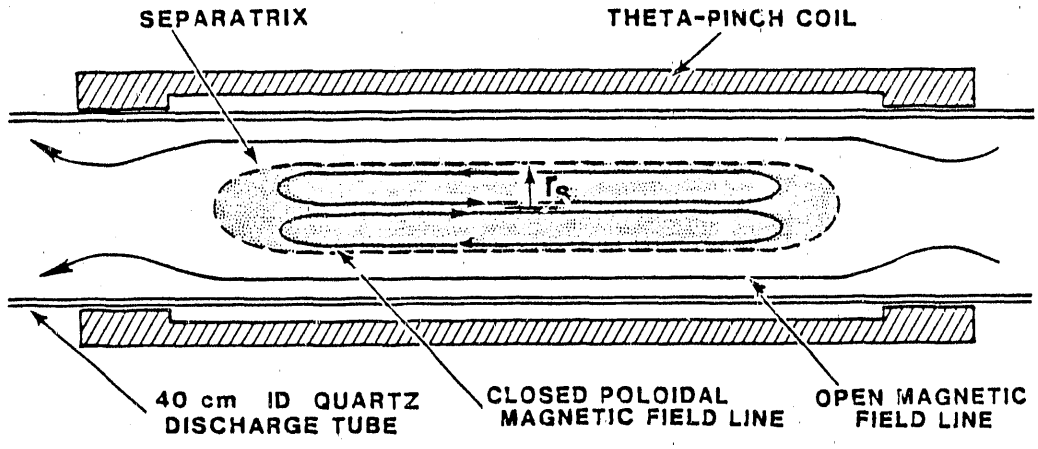

Figure 1: The field-reversed configuration (FRC).

pinch coil, which can be shaped to provide end mirrors for axial centering or constructed with a small cone angle to translate the plasma into an adjoining chamber. The vacuum vessel is an insulating quartz tube which allows penetration of the fast-rising magnetic field. The FRC itself is axially elongated (prolate); its field lines are primarily straight (axial) with their curvature concentrated near the ends. In the absence of toroidal field, there exists a magnetic field null at radius $R = r_s/\sqrt{2}$, where r_s is the separatrix radius at the midplane. Outside the separatrix the FRC is surrounded by an open field line sheath, which is several ion gyroradii in radial thickness, formed by the axially escaping plasma.

The combination of radial and axial equilibrium for the simple prolate geometry

of the FRC yields a profile-independent relation for the plasma β averaged over the FRC cross section. This average β relation is $<\beta> = 1 - x_s^2/2$ where $x_s = r_s/r_c$ is the separatrix radius normalized by the coil radius. From this relation, one can see that $\beta = 0.8 - 1$ for typical values of x_s (β is defined in terms of the excluded magnetic pressure near the coil).

The parameter s is a measure of the MHD-like character of the FRC. It can be expressed as $s = a/<\rho_i>$, where $a = r_s/4$ is the effective radial scale length and $<\rho_i>$ is the gyroradius of a thermal ion in the average internal field. Most FRCs studied so far have s in the range 1–2 in the regime where ion kinetic effects are important, while s values of 10–40 are needed for an FRC reactor.[1,3] The need to increase s in order to improve confinement forces the FRC into the MHD regime in which numerous instabilities are predicted.[1]

II. Global Power Flow in FRCs

The elongated high-β equilibrium of the FRC greatly simplifies the measurements required to assess gross confinement behavior. As a result, the global power flow of the FRC is rather well characterized. On the other hand, the relatively thick plasma layer on the open field lines controls the particle outflow in present FRCs and obscures the physics of particle confinement in the closed field region.

An illustration of the data used to assess the global power flow is shown in Figure 2 for a series of 3 mtorr FRCs, representing the best operating condition in the Large Source Modification[4] of the FRX-C device at Los Alamos, herein denoted as LSM. These FRCs were formed with initial bias field B_b = 650–750 G and crowbarred magnetic field B = 4.2–4.6 kG. The radius and volume are obtained from a spline fit to the excluded flux radius profile at each time step. The particle inventory is estimated as $N = \bar{n}V$ where $\bar{n} = \int n\, dl/2r_s$ and V is the separatrix volume; measurements of the radial density profile show that $\bar{n}$ is an excellent approximation to the average density within the separatrix when the FRC is cylindrically symmetric. The symmetry assumption is violated after 80 μs by the growth of the $n = 2$ rotational instability, hence there are erroneous oscillations in N caused by variations in interferometer path length through the FRC as the mode rotates. The influence of residual asymmetries

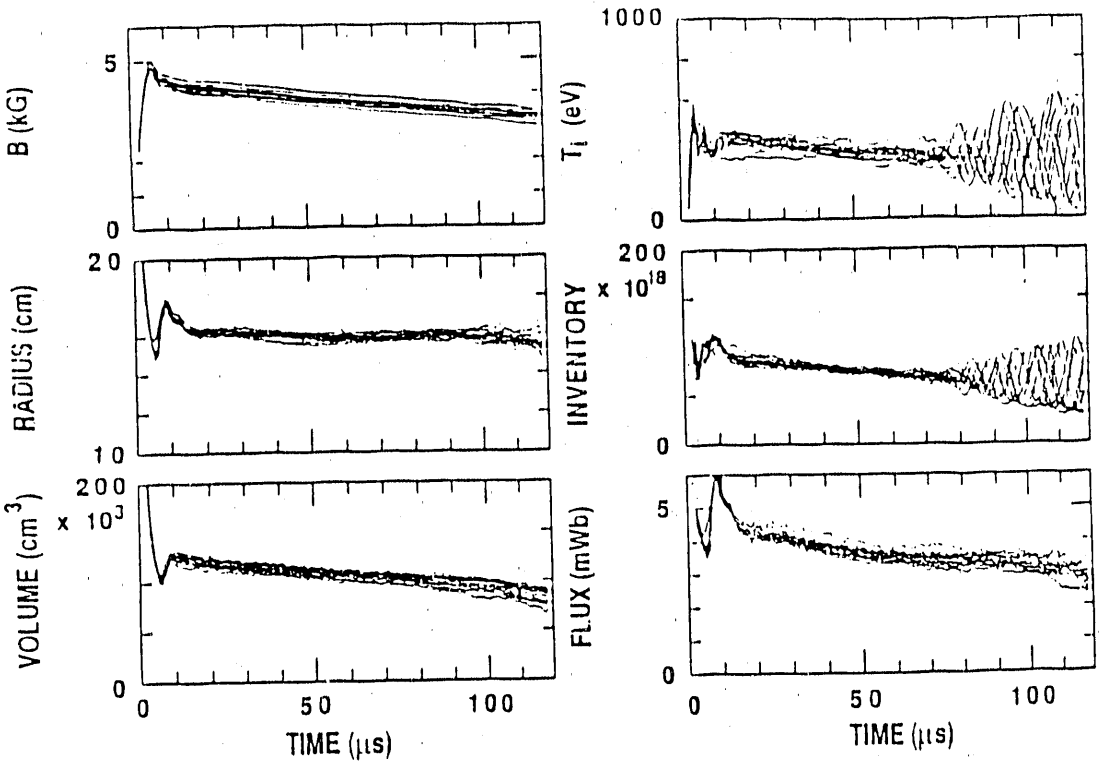

Figure 2: Time evolution of a series of 3 mtorr, reduced-field FRCs.

during the equilibrium evolution (arising from, for example, the $n = 1$ wobble mode[23]) is reduced by averaging an ensemble of similar FRCs. The ion temperature is estimated from the radial pressure relation $T_i + T_e = <\beta> B^2/(2\mu_o \bar{n})$ together with Thomson scattering measurements which indicate a constant $T_e = 140 \pm 30$ eV for this condition. The poloidal flux of the FRC is estimated using a typical diffuse profile model[1,8] for the internal magnetic profile ($\phi = \pi r_c^2 B(x_s/\sqrt{2})^{3.25}$). The flux estimate is subject to uncertainties due to the profile model as well as nonequilibrium effects (seen as oscillations in ϕ during formation).

After FRCs are heated during formation by a combination of shock, magnetic compression and flux dissipation heating, they evolve during the equilibrium phase with losses which greatly exceed the power inputs from adiabatic compression and ohmic heating. A plasma energy decay time which neglects the equilibrium heating terms is occasionally quoted in the FRC literature. The more fundamental energy *confinement* time is defined as $\tau_E = E_p/(P_{C_p} + P_\Omega - \dot{E}_p)$ where P_{C_p} and P_Ω are the compression and ohmic heating power, respectively, and E_p is the plasma energy within the separatrix. In most magnetic confinement systems, determination of τ_E requires time-dependent

profile information in order to accurately assess the power inputs. However it has been shown[5] that the *combination* of compression and ohmic power inputs is insensitive to profile changes because of equilibrium constraints in the FRC. As a result, τ_E can be obtained solely from time-dependent external measurements of the separatrix radius profile and the magnetic field by the expression[5]

$$\frac{1}{\tau_E} = \frac{5/3}{\tau_V} + \frac{2}{\tau_B} + 2\frac{1 - <\beta>}{<\beta>}\left(\frac{1}{\tau_r} + \frac{2/3}{\tau_B}\right)$$

where τ_V, τ_B, and τ_r are the exponential decay times for V, B, and r_s, respectively. The decay times needed to determine τ_E are evaluated during the FRC equilibrium (20–80 μs in Figure 2); little error is introduced by using a time-averaged value for $<\beta>$. Thus τ_E can be accurately determined and is routinely available on every FRC discharge.

The zero-dimensional power flow can be established[5] from the energy equations:

$$\dot{E}_{pe} = P_{ce} + P_{\Omega e} + P_{eq} - L_{Ce} - L_{NCe}$$

$$\dot{E}_{pi} = P_{ci} + P_{\Omega i} - P_{eq} - L_{Ci} - L_{NCi}$$

where P_c is the compression heating power, P_Ω is the ohmic heating power, P_{eq} is the equilibration power flowing from the ions to the electrons, L_C is the power loss associated with particle transport, L_{NC} is the power loss associate with all other loss processes (thermal conduction, charge exchange, and radiation), and the subscripts denote electrons or ions. The compression heating terms are related to the change in volume ($P_{c(e,i)} = (2/3)(E_{p(e,i)}/\tau_V)$). The ohmic heating is given by $P_\Omega = E_p/\tau_\Omega$ where $\tau_\Omega = (3/4)(<\beta>/(1 - <\beta>))\tau_\phi$ and τ_ϕ is the flux confinement time. A fraction $\epsilon = 0.7 - 0.3(T_e/T_i)$ of P_Ω is estimated to be deposited to the ions based on classical plus lower-hybrid-drift resistivity. The equilibration power is given by $P_{eq} = ((T_i - T_e)/(T_i + T_e))(E_p/\tau_{eq})$ where τ_{eq} is the electron-ion equilibration time. The convective power loss term, $L_{C(e,i)} = (5/3)(E_{p(e,i)}/\tau_N)$, is based on an energy loss of $(5/2)k_BT$ per particle. The choice of 5/2 as the particle convection coefficient seems appropriate for the FRC, since one can identify k_BT of compressional work on the FRC for each particle lost.[6] This model is used to evaluate the nonconvective loss terms based on measurements of the other quantities.

The global power flow for the 3 mtorr FRCs in LSM, evaluated at the middle of the equilibrium, is shown in Figure 3. The dominant loss term is particle convection.

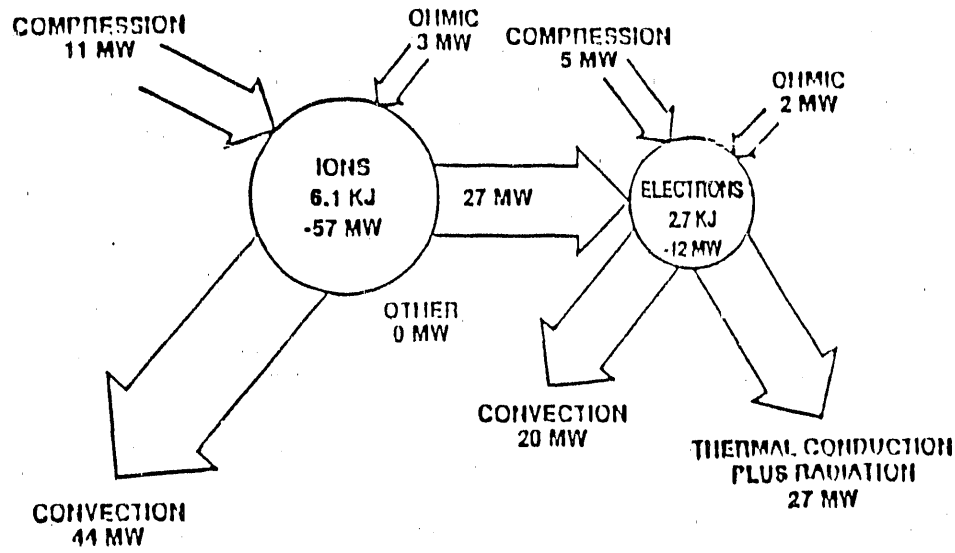

Figure 3: Zero-dimensional power flow analysis of 3 mtorr FRCs shown in Figure 2.

accounting for 70% of the losses. The remaining 30% of the power loss appears in the electron nonconvective channel. Of these electron losses, radiation is expected to be small in view of the moderately high plasma density ($\approx 10^{15}$ cm^{-3}) and brief period of wall contact (≈ 1 μs during formation); this expectation has been verified in cases where radiation losses have been measured.[7] The power flow analysis suggests that the nonconvective *ion* losses are negligible. This result is consistent with the absence of particle refueling in FRCs (except possibly during FRC translation into a static gas fill) and the absence of a cold boundary near the separatrix to drive ion thermal conduction. Unlike other magnetic confinement systems, the ratio of plasma energy to magnetic energy within the FRC separatrix ($E_p/E_B = (3/2)<\beta>/(1-<\beta>)$) is much greater than unity; thus Ohmic dissipation must be a small heating term in equilibrium. The energy confinement time for this condition is 100 μs, while τ_p and τ_N are 225 μs and 250 μs, respectively. Compared with R^2/ρ_{ie} scaling[9] (where ρ_{ie} is the thermal ion gyroradius in the external field), an often-used benchmark similar to the predictions of a transport theory[10] based on lower hybrid drift resistivity, τ_N exceeds the scaling prediction by about 50%.

III. Profile Measurements and Local Transport Coefficients

A limited number of FRC profile measurements have been performed and used to estimate local transport coefficients. An electron temperature profile was measured for 5 mtorr FRCs in FRX-C,[11] and two point profiles (field null and symmetry axis) were obtained in LSM.[12] These profiles were obtained from single point and time Thomson scattering measurements. Electron density profiles have been more frequently reported.[14–17] These profiles have been obtained by unfolding line-integral density profiles from interferometer arrays consisting of 2 to 7 chords. This profile determination has been aided in some cases by exploiting the $n = 1$ wobble motion of the FRC.[23]

The available electron temperature profile information shows that $T_e(r)$ is relatively flat inside the separatrix, with T_e dropping by 10–20% between R and r_s. The temperature gradients measured in LSM, for 2–4 mtorr FRC with medium bias field ($B_b \approx 600$ G), have been interpreted in terms of electron thermal diffusivities,[12] using a simple linear profile and assuming $T_e(r_s) = T_e(0)$. The results are shown in Table 1, together with calculated values for classical and Bohm diffusivities. This comparison

Table 1: Rough estimates of electron thermal diffusivities.

p_o (mtorr)	s	$\chi_{\perp e}$ (m^2/s)	$\chi_{\perp cl}$ (m^2/s)	χ_{Bohm} (m^2/s)
2	1.3	350	3.4	79
3	1.2	295	5.3	89
4	1.9	770	5.4	67

shows that the $\chi_{\perp e}$ values, while high, represent transport anomalies with respect to classical diffusivity which are no more than those present in tokamak discharges. On the other hand, the estimated diffusivities are several times worse than Bohm. The thermal diffusivity is observed to double as the fill pressure is raised from 3 to 4 mtorr.

A line-integral density profile and the deduced radial density profile[17] are illustrated in Figure 4 for a 3 mtorr FRC in LSM similar to those in Figure 2. The data are obtained from a six chord 3.39 μm HeNe interferometer array. The density profile is

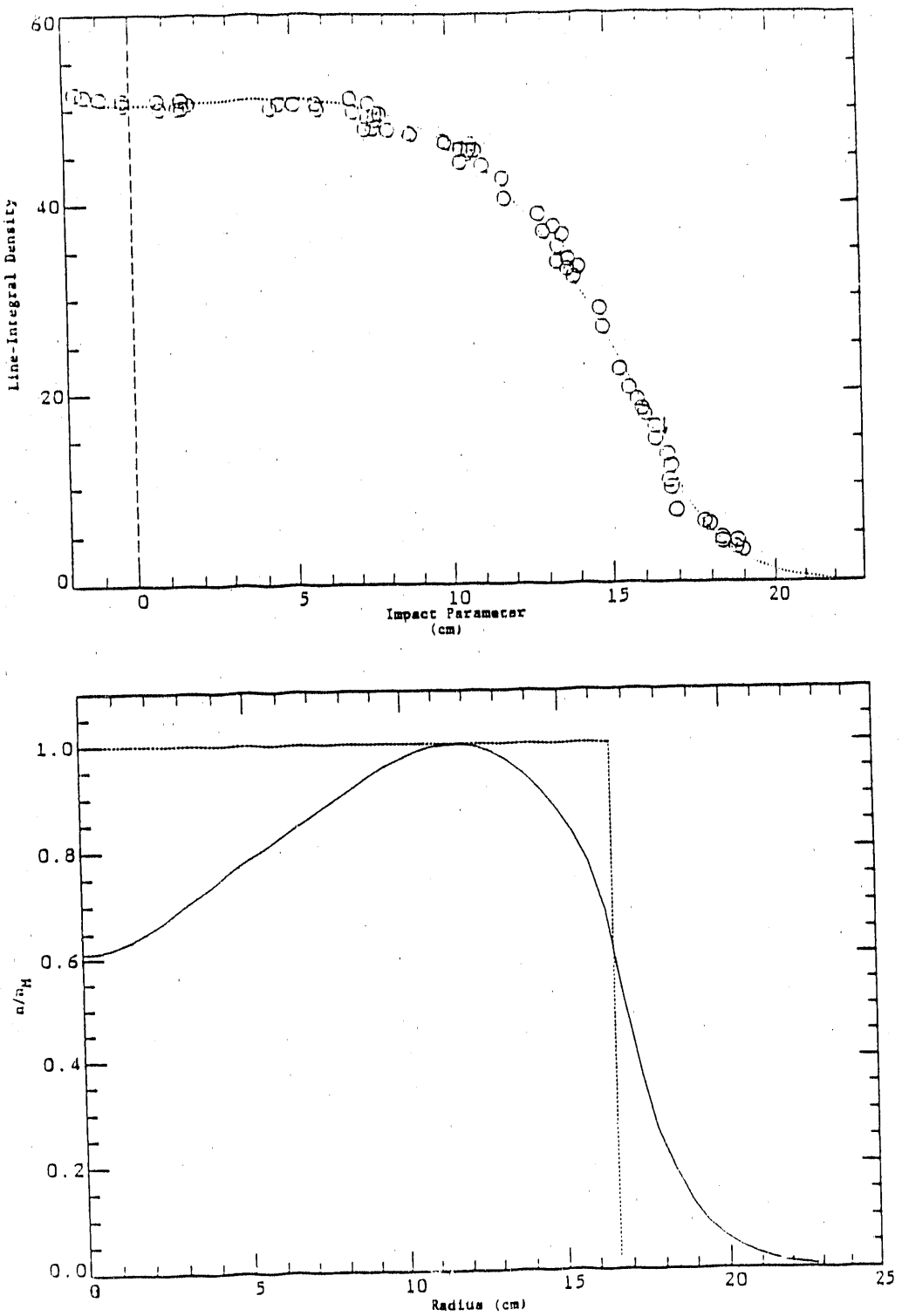

Figure 4: (a) Composite line-integral density profile for a 3 mtorr FRC as a function of impact parameter. (b) Inferred radial density profile obtained from fit to data in (a).

inferred by fitting a model profile consisting of a truncated rigid-rotor profile inside the separatrix and an exponential decay outside. An offset parameter is included in the fitting procedure to account for rigid motions of the FRC perpendicular to the interferometer chords. The composite profile shown in Figure 4(a) is formed by adjusting the nominal impact parameters of the interferometer array to reflect the offset each time step during the FRC equilibrium. The profile (Figure 4(b)) shows fairly high density on the separatrix (60% of the density at the field null) and a gradual falloff outside the separatrix (density scale length $a_n \approx 2$ cm).

Considerable information can be extracted when the density profile is combined with a model for the temperature profiles.[15] For this purpose, $T_e(r)$ is taken to be flat for $r < r_s$ and drop outside the separatrix with a scale length similar to the density (consistent with the measured $T_e(r)$ profile). $T_i(r)$ is taken to be flat everywhere, as expected for $s \leq 2$ FRCs and in agreement with $1\frac{1}{4} - D$ transport calculations.[13] Using this model, one can estimate $<\beta>$, the separatrix β (β_s), and the scale length for β at $r \geq r_s$ (a_β). In addition, one can estimate the separatrix resistivity $\eta(r_s)$ (from the measured τ_N and a_β) and the lower hybrid drift resistivity at r_s. The resistivities (based on the profile) are shown in Table 2 for 3–4 mtorr medium bias FRCs in LSM.[17] This comparison indicates, for the 3 mtorr case, that $\eta(r_s)$ exceeds η_{cl} by a factor 14

Table 2: FRC resistivities deduced from line-integral density profile modelling.

p_o (mtorr)	s	$\eta(r_s)$ ($\mu\Omega\, m$)	$\eta(R)$ ($\mu\Omega\, m$)	η_{LHD} ($\mu\Omega\, m$)	η_{cl} ($\mu\Omega\, m$)
3	1.4	13 ± 5	7.9	5.1	0.9
4	2.1	29 ± 10	18.1	1.9	0.9

and η_{LHD} by a factor 2.5. For the 4 mtorr case, the expected improvement in particle confinement from a reduction in η_{LHD} is not observed; instead τ_N drops and $\eta(r_s)/\eta_{LHD}$ increases to 15. One should note that the standard transport model[10] predicts that $w = a_n/\rho_{ie}$ should be about unity; η_{LHD} based on the measured profile with $w = 3$–4 is much lower than the one predicted within the transport model. The table also includes estimates for $\eta(R)$ based on a rigid-rotor profile for the magnetic field; this estimate

indicates that $\eta(R)$ is 9 and 20 times classical for the 3 and 4 mtorr cases, respectively.

IV. Confinement Limitations and Axial Dynamics

Although the smaller FRC machines have been able to operate over a wide range of fill pressure and initial bias field, it has been observed that the operating range in which relatively good confinement can be achieved becomes more restricted—and little overall improvement in confinement is obtained—as the machine size increases. This trend is especially clear in the results from the LSM device at Los Alamos. The dependence of τ_ϕ on fill pressure in LSM is illustrated in Figure 5. It is observed that

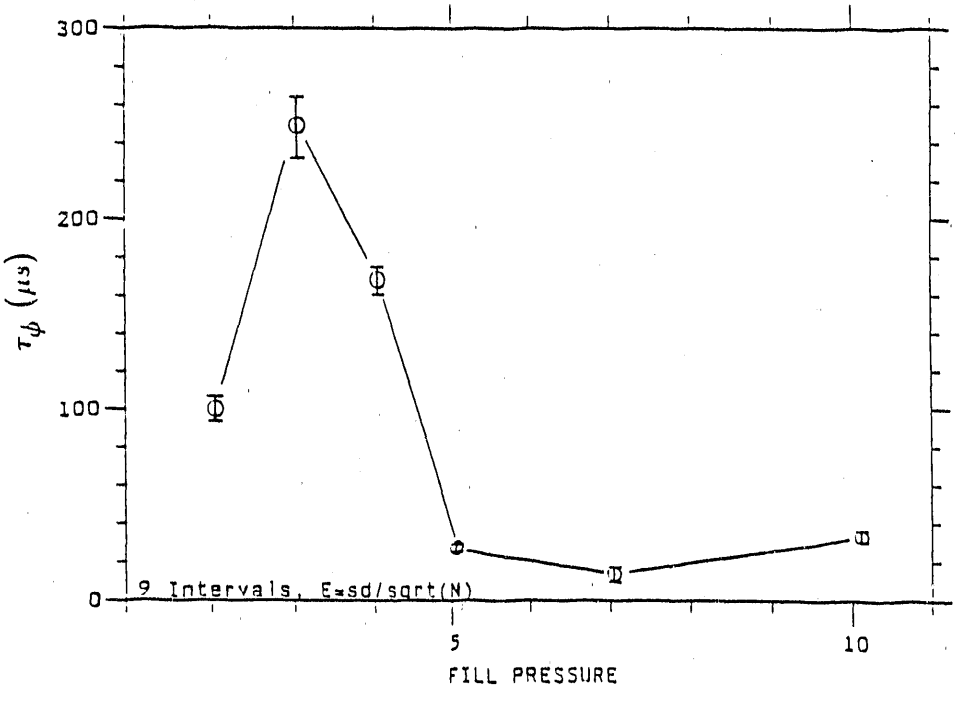

Figure 5: Dependence of τ_ϕ on fill pressure in LSM.

the available operating range is only 2–4 mtorr, with some degradation in confinement already occuring at the upper end of that range. The 5 mtorr case is discussed in detail in a companion lecture presented at this school[2] and shows clear evidence of the tilt instability. The flux confinement shown for 5 mtorr is somewhat misleading, because most of flux is lost abruptly just after the time of the instability.

For a given fill pressure, a further limitation on confinement is imposed by the bias

field strength used to form the FRC. This limitation is illustrated, again in terms of τ_ϕ, for 3 mtorr FRCs in LSM (Figure 6). The flux confinement initially increases with bias field, but then drops as the bias field is raised above about 800 G. This transition has

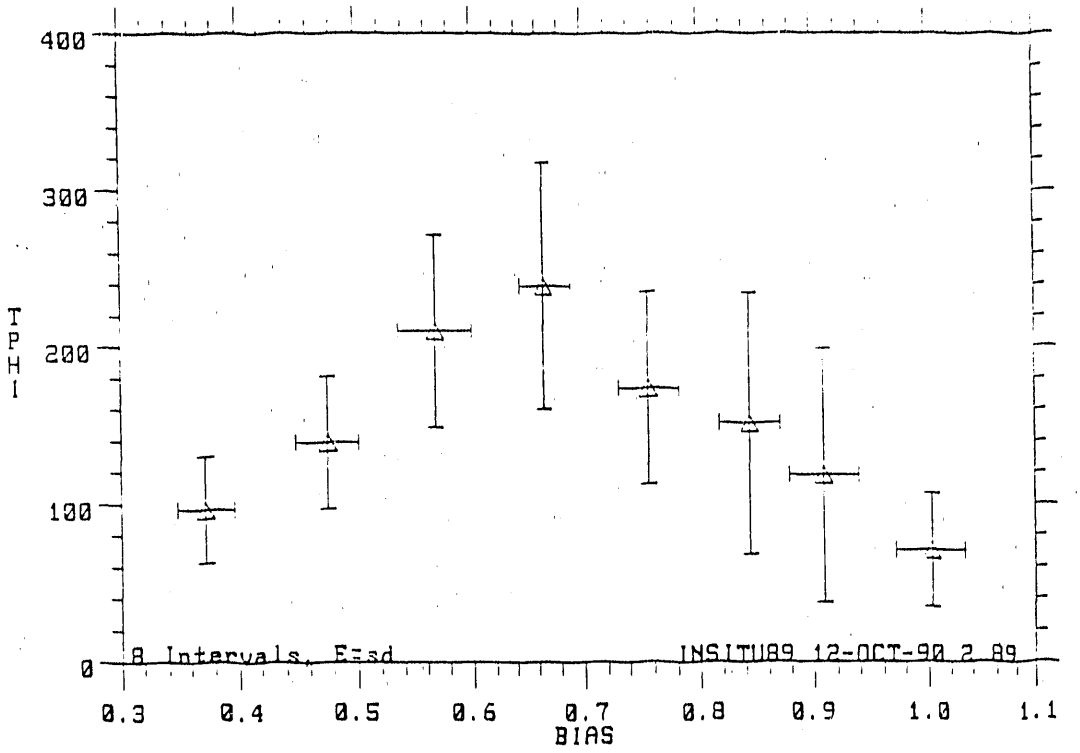

Figure 6: Dependence of τ_ϕ on bias field for 3 mtorr FRCs in LSM.

been examined in detail for another experimental run in which Thomson scattering T_e data is available;[18] the results are summarized in Table 3. The poloidal flux ϕ_p, r_s, and $T_e(R)$ all increase with bias field, suggesting no discontinuity in the formation characteristics. The field null resistivity remains constant at low and medium bias fields, but increases abruptly at high bias. The resistivity anomaly $\eta(R)/\eta_{cl}$ is 10 to 15 at low and medium bias, increasing to about 50 at high bias. No evidence of classical resistivity scaling is present.

The degradation in confinement with increasing bias field has been correlated with the presence of strong axial dynamics during formation. Axial dynamics occur when the bias field is large enough that the field line tension at the ends of the FRC exceeds the plasma pressure at the time of field line connection; for nontearing formation (as in LSM) this time occurs when the plasma lifts off the wall during radial implosion. Further increase in bias field leads to axial shock and a transiently short FRC.

Table 3: Bias scan for 3 mtorr FRCs in LSM.

Parameter	Units	Low bias	Medium Bias	High Bias
B_b	G	440 ± 50	650 ± 30	860 ± 20
B	kG	3.9 ± 0.1	4.1 ± 0.2	4.1 ± 0.1
r_s	cm	11.1 ± 0.9	15.4 ± 0.9	18.6 ± 0.6
V	liter	59 ± 9	107 ± 10	143 ± 8
ϕ_p	mWb	1.1 ± 0.4	3.5 ± 0.7	6.3 ± 0.8
s		0.6 ± 0.1	1.3 ± 0.2	1.9 ± 0.2
$\bar{n}$	10^{14} cm^{-3}	8.3 ± 0.6	7.2 ± 0.6	6.0 ± 0.5
$T_e(R)$	eV	120 ± 20	158 ± 20	194 ± 42
τ_ϕ	μs	120 ± 50	214 ± 68	130 ± 60
$\eta(R)$	$\mu\Omega\, m$	9 ± 4	9 ± 3	25 ± 14
η_{cl}	$\mu\Omega\, m$	0.9 ± 0.3	0.6 ± 0.2	0.5 ± 0.2

The best correlation found between confinement and axial dynamics[19,22] is illustrated in Figure 7 which includes 2–4 mtorr LSM data with bias field exceeding 600 G and also 5 mtorr FRX-C data with a reduced τ_ϕ scale to account for their smaller radius. Since the axial dynamics should be related to the *change* in FRC elongation, we define an inverse shock strength e_{md}/e_M where e_{md} and e_M are the minimum and maximum elongations, respectively. The excluded flux array is ineffective in measuring the length of short FRCs, so the minimum length used in e_{md} is measured using an axial interferometer array; e_M is estimated by $l_{coil}/2r_s$. One sees a clear trend in all the data sets for τ_ϕ to decrease when e_{md} becomes small.

Many studies were conducted in an attempt to relate the confinement degradation to some formation problem, but no conclusive connection could be established.[22] The outcome of these formation studies motivated a search for signatures of various MHD modes which have been predicted to be unstable in the FRC, especially the $n = 1$, $m = 1$ internal tilt mode.

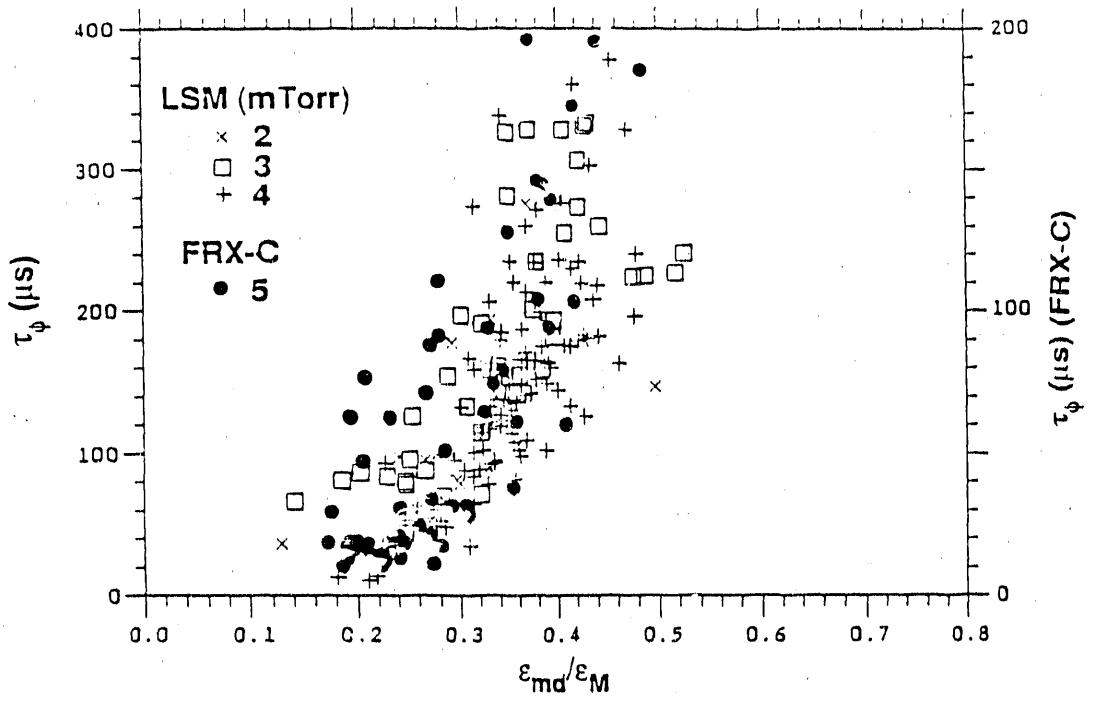

Figure 7: Variation of τ_ϕ in LSM (r_{coil} = 0.35 m) and FRX-C (r_{coil} = 0.25 m) with inverse shock strength.

V. Confinement and Tilt Amplitudes

The experimental search for tilt modes was conducted using a Mirnov loop array consisting of 64 external B_θ pickup loops (8 axial × 8 toroidal) located just inside the coil.[20] Some of the results obtained with this diagnostic, and a detailed comparison between experimental data for 5 mtorr FRCs in LSM and MHD calculations, are discussed in a companion lecture.[2] This comparison shows good agreement between theory and experiment in all features and establishes that the $n = 1$, axially odd components observed by the array are signatures of the tilt instability.[21] In light of this observation, it is not surprising that the regime of relatively good confinement has been restricted to low values of s ($s \leq 2$), in the regime where the tilt is suppressed by kinetic effects. More precisely, finite larmor radius theory[24] applied to the FRC tilt mode predicts stability for $s/e \leq 1/4$, where e is the FRC elongation. This prediction agrees fairly well with the measured peak tilt amplitudes, which are limited to less than 5 G for $s/e < 0.3$ but which increase to several tens of gauss at higher s/e.

The correlation between confinement degradation and maximum tilt amplitude is

best shown by the variation of the resistivity anomaly at the field null $\eta(R)/\eta_{cl}$ (Figure 8). The resistivity anomaly is observed to grow with tilt amplitude until the amplitude

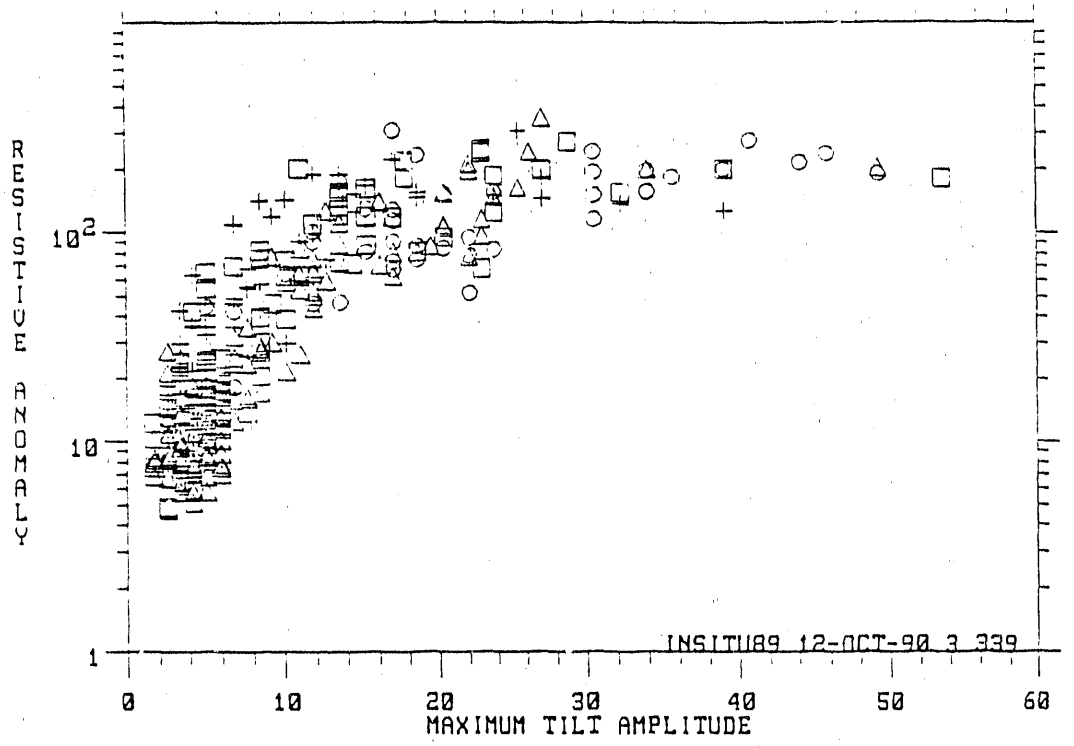

Figure 8: Variation of $\eta(R)/\eta_{cl}$ with maximum tilt amplitude for 2–5 mtorr FRCs in LSM.

reaches about 15 G. At the higher amplitudes the flux does not decay smoothly but decreases abruptly after the maximum tilt growth; the diagnostics suggest that closed field confinement is lost soon after that time. Thus the τ_ϕ values used to calculate the resistivity anomaly are not meaningful for large tilt events.

The evidence for the tilt instability and its dependence on s/e are consistent with the correlation between confinement and axial dynamics. In the low s regime, the normalized growth rate γ/γ_{MHD} for the tilt increases with s,[25] while $\gamma_{MHD} \approx 2v_i/l_s$ varies inversely with e. Raising the bias field increases $s = a/<\rho_i>$ by increasing a and the average internal B, and drives axial shocks resulting in a transiently small e by increasing the field line tension; viscosity can also keep those FRCs short after formation. Raising the fill pressure increases s by reducing T_i; in addition, axial dynamics are difficult to avoid for $p_o > 4$ mtorr in LSM for reasons that remain unclear. In either case the larger values of s/e lead to more MHD-like behavior, greater predicted growth rate for the tilt instability, and enhanced tilt amplitudes which are deleterious

to confinement.

VI. Magnetic Compression Heating Experiments

The relatively low main fields which have been characteristic of FRC formation in modern experiments have also limited the temperatures to $T_i + T_e < 1$ keV. Confinement at higher temperature can been studied by exploiting the translation capability of FRCs to perform relatively efficient magnetic compression heating in an adjacent, smaller radius, and lower-voltage theta pinch coil. This program has been carried out in the FRX-C/LSM facility at Los Alamos. Results from these compression experiments[26] indeed show substantial heating to $T_i + T_e \leq 2$ keV, but with confinement decreasing commensurate with the reduction in r^2.

The experimental arrangement is shown schematically in Figure 9. FRCs are formed

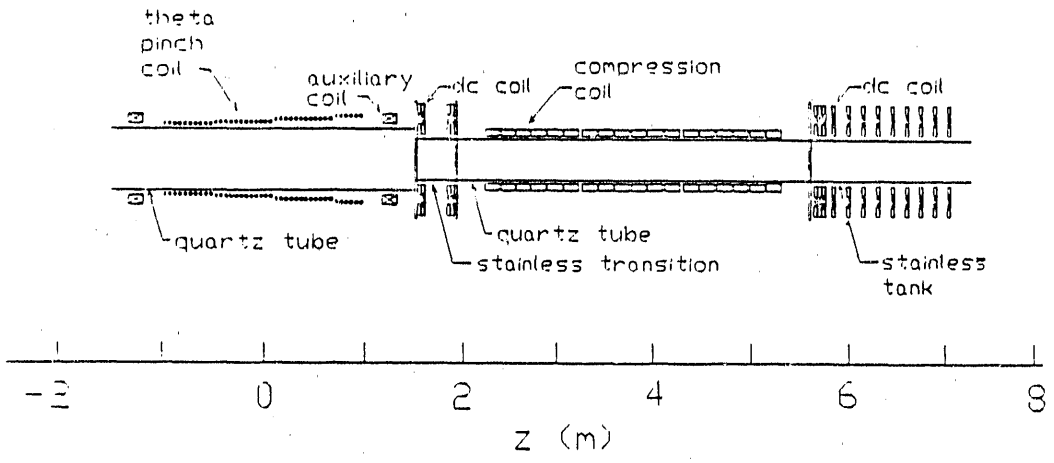

Figure 9: Schematic diagram of the LSM device modified for high-power FRC compression heating experiments.

in a tapered theta pinch coil using a 3 mtorr-equivalent puffed deuterium fill, translated through a dc coil transition region, enter the compression region, reflect from a dc mirror field, and are trapped in the compressor. The compression coil is 0.46 m in diameter and 3 m long; the quartz tube within it has a diameter of 0.4 m. The details of the 10 kV, 5 MA ignitron-switched compression system power supply are available elsewhere.[27]

During compression, B is raised from the guide field value to 18 kG in 55 μs. Two

modes of operation have been employed. The higher temperature mode is obtained by forming FRCs with the full θ-pinch main bank, translating into a 0.4 T guide field, and compressing as soon as the FRC has fully entered the compressor (about 30 μs). In this case, the plasma energy is tripled (from 5 to 15 kJ), with neutron yields up to 10^9, and $n_e = 3 \times 10^{15}$ cm^{-3}; however τ_E is limited to about 30 μs or less. For these high-temperature conditions, quadrupole stabilization field of up to 4% B is found to be insufficient to control the $n = 2$ rotational mode; this mode often terminates the FRC prior to peak compression. Ion temperatures (Figure 10(a)) are estimated from absolutely calibrated neutron rate measurements assuming Maxwellian fusion reactivity, and also from radial pressure after subtracting the measured $T_e(0)$ (Figure 10(b)). The T_i measurements agree well for the highest fields obtained, indicating $T_i = 1.5$ keV. However the neutron T_i estimate is significantly higher than the pressure balance T_i (which measures the perpendicular temperature) at lower field. This difference is especially pronounced for full compression voltage, and represents an enhancement in neutron rate of about a factor of ten which is much larger than the calibration uncertainty of about 50%. The apparent enhancement in parallel over perpendicular heating is consistent with with the relatively long equipartition time ($> 20\mu$s) and suggests the presence of nonadiabatic (or double adiabatic[28]) heating effects. The Thomson scattering measurements show substantial electron heating up to $T_e = 0.4$ keV with a scaling close to the $B^{4/5}$ adiabatic prediction.

A second series of compression experiments were performed on FRCs formed with somewhat reduced main field (similar to the best 3 mtorr conditions), translated into a reduced guide field (0.2 T), and allowed to settle (to permit more accurate confinement measurements) prior to initiating compression at 100 μs. Significant heating is again observed, similar to adiabatic scaling, in spite of substantial particle loss. The inferred τ_N and τ_ϕ remain approximately equal during compression, decreasing roughly in agreement with r^2 scaling from about 140 to 33 μs. The confinement times for the compressed FRCs are similar to those obtained on smaller devices with comparable plasma parameters.[29]

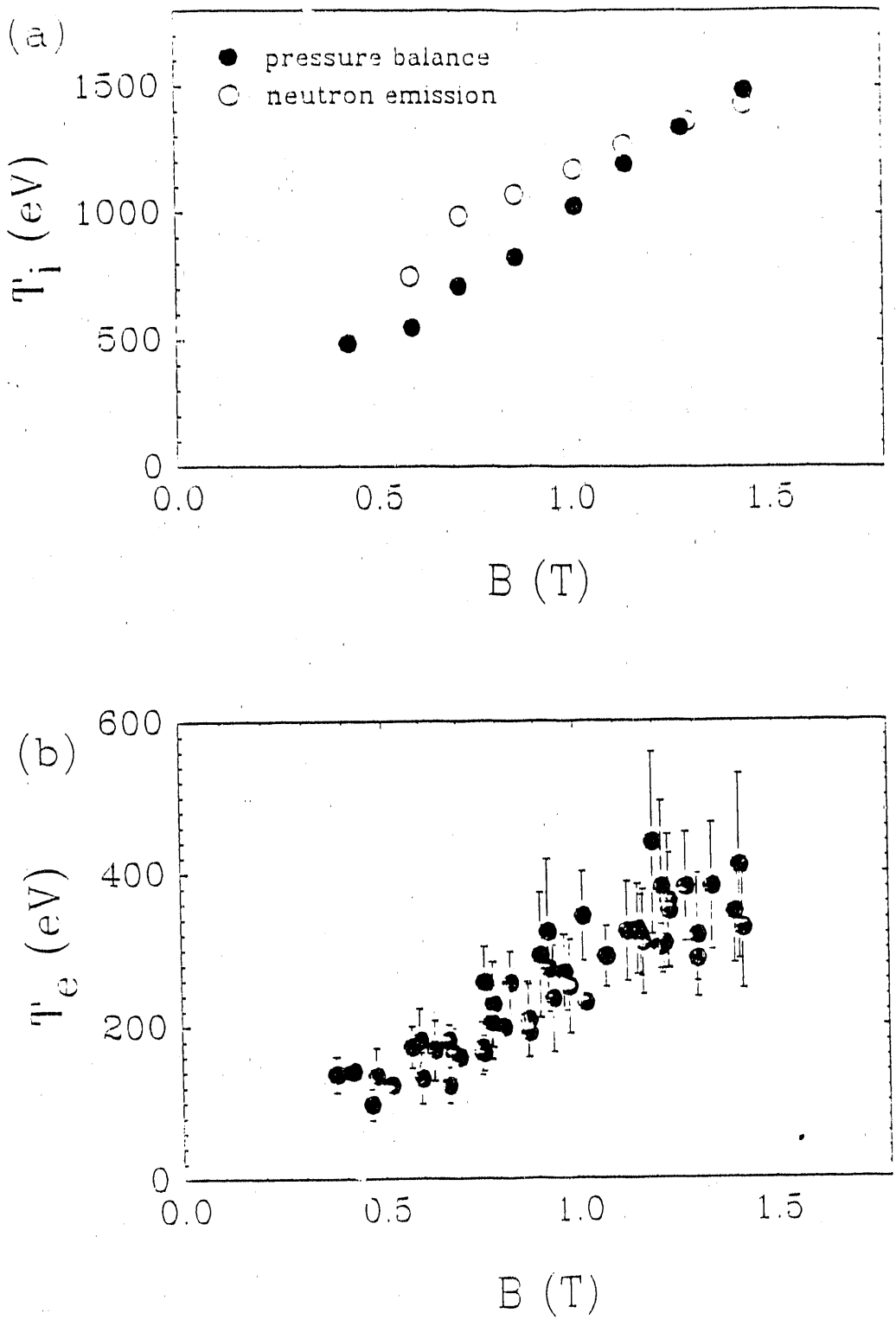

Figure 10: Variation of (a) T_i and (b) T_e with compression field. The T_i data are averages from pressure balance and the neutron rate. The T_e data represent single-point Thomson scattering measurements at $r = 0$ for 64 separate discharges.

Acknowledgements

The author wishes to thank all past and present members of the Los Alamos FRC group for their contributions to the work reported here, especially the primary role of Dr. M. Tuszewski in the stability experiments and Dr. D. J. Rej in the compression heating experiments. FRC research at Los Alamos is funded by the U. S. Department of Energy.

References

[1]M. Tuszewski, Nucl. Fusion **28** (1988) 2033.

[2]D. C. Barnes, these proceedings.

[3]W. Kernbichler, *et al.*, *$D-^3He$ in Field-Reversed Configurations—RUBY, An International Reactor Study*, in 13th International Conference on Plasma Physics and Controlled Nuclear Fusion Research (Washington, D.C., 1990) paper CN-53/G-2-3.

[4]R. E. Siemon, *et al.*, in Plasma Physics and Controlled Nuclear Fusion Research 1988 (Proc. 12th Int. Conf. Nice, 1988), Vol. 2, IAEA, Vienna (1989) 517.

[5]D. J. Rej and M. Tuszewski, Phys. Fluids **27** (1984) 1514.

[6]S. Hamada, Nucl. Fusion **26** (1986) 729.

[7]R. E. Siemon, *et al.*, in Plasma Physics and Controlled Nuclear Fusion Research 1984 (Proc. 10th Int. Conf. London, 1984), Vol. 2, IAEA, Vienna (1985) 511.

[8]R. L. Spencer, M. Tuszewski, R. K. Linford, Phys. Fluids **26** (1983) 1564.

[9]K. F. McKenna, *et al.*, Phys. Rev. Lett. **50** (1983) 1787.

[10]M. Tuszewski, R. K. Linford, Phys. Fluids **25** (1982) 765.

[11]D. J. Rej, W. T. Armstrong, Nucl. Fusion **24** (1984) 177.

[12]D. J. Rej, *et al.*, Nucl. Fusion **30** (1990) 1087.

[13]K. A. Werley, Phys. Fluids **30** (1987) 2129.

[14]M. Tuszewski, Plasma Phys. Contr. Fusion **26** (1984) 991.

[15]R. E. Chrien, S. Okada, Phys. Fluids **30** (1987) 3574.

[16]S. Okada, Y. Kiso, S. Goto, T. Ishimura, J. Appl. Phys. **65** (1989) 4625.

[17]R. E. Chrien, 9th U. S. Compact Toroid Symposium (Union, WA, 1989) 110.

[18]D. J. Rej, *et al.*, Phys. Fluids B **2** (1990) 1706.

[19]M. Tuszewski, *et al.*, in Proceedings of the 8th U. S. Compact Toroid Symposium and 9th US-Japan Workshop on Compact Toroids (College Park, MD) University of Maryland (1987) 191.

[20]M. Tuszewski, *A Mirnov Loop Array for Field-Reversed Configurations*, Rev. Sci. Instr. **61** (November 1990).

[21]M. Tuszewski, *et al.*, *Observation of Tilt Instabilities in Field-Reversed Configurations*, submitted to Phys. Rev. Lett. (1990).

[22]M. Tuszewski, *et al.*, *Axial Dynamics in Field Reversed Theta Pinches. I. Formation*, to be submitted to Phys. Fluids B (1990).

[23]M. Tuszewski, *et al.*, *The $n = 1$ Rotational Instability in Field-Reversed Configurations* Phys. Fluids B **2** (October 1990).

[24]M. N. Rosenbluth, *et al.*, Nucl. Fusion Suppl. (1962) 143.

[25]D. C. Barnes, *et al.*, Phys. Fluids **29** (1986) 2616.

[26]D. J. Rej, *et al.*, *Tilt Stability and Compression Heating Studies of Field-Reversed Configurations*, 13th International Conference on Plasma Physics and Controlled Nuclear Fusion Research (Washington, D.C., 1990) paper CN-53/C-4-4.

[27]D. J. Rej, *et al.*, LA-11519-MS (1989).

[28]R. L. Spencer, Proceedings of Sherwood Theory Meeting (Madison, WI) University of Wisconsin, Madison (1985) paper 1Q-8.

[29]J. T. Slough, A. L. Hoffman, Nucl. Fusion **26** (1986) 1693.

END

DATE FILMED

11 / 21 / 90